Deformation analysis of vesicles in an alternating-current electric field

Yu-Gang Tang,[1] Ying Liu,[1,*] and Xi-Qiao Feng[2]

[1]*Department of Mechanics, School of Civil Engineering, Beijing Jiaotong University, Beijing 100044, People's Republic of China*

[2]*AML and CNMM, Department of Engineering Mechanics, Tsinghua University, Beijing 100084, People's Republic of China*

(Received 18 March 2014; revised manuscript received 4 June 2014; published 13 August 2014)

In this paper the shape equation for axisymmetric vesicles subjected to an ac electric field is derived on the basis of the liquid-crystal model. The equilibrium morphology of a lipid vesicle is determined by the minimization of its free energy in coupled mechanical and ac electric fields. Besides elastic bending, the effects of the osmotic pressure difference, surface tension, Maxwell pressure, and flexoelectric and dielectric properties of phospholipid membrane as well are taken into account. The influences of elastic bending, osmotic pressure difference, and surface tension on the frequency-dependent behavior of a vesicle membrane in an ac electric field are examined. The singularity of the ac electric field is also investigated. Our theoretical results of vesicle deformation agree well with previous experimental and numerical results. The present study provides insights into the physical mechanisms underpinning the frequency-dependent morphological evolution of vesicles in the electric and mechanical fields.

DOI: 10.1103/PhysRevE.90.022709 PACS number(s): 87.16.D−, 87.10.Hk, 61.30.Dk, 77.84.Nh

I. INTRODUCTION

Living cells, including those in our bodies, are often subjected to electric and magnetic fields of different intensities and frequencies, which may result from sources such as mobile phones, home appliances, and power transmission lines [1]. In response to surrounding electric fields, biological cells continuously alter the properties (dielectric and electric conductivities and polarization) of their cell membranes to maintain their normal physiological functions [2]. Weak electric fields influence biological processes of cells, e.g., signal transition, wound healing, migration, and spreading [3]. Strong electric fields can produce electroporation in cell membranes, which enables delivery of foreign genes, proteins, antibodies, and drugs into cells [4,5]. In addition, the mechanical-electrical coupling effects have been utilized to develop novel techniques for the control and manipulation of cells. Obviously, understanding the morphological evolution of vesicles under electric fields is an issue of extensive interest.

Recently, much effort has been directed toward investigating the influence of electric fields on vesicle deformation. Kakorin *et al.* [6] analyzed the electroporative deformation of lipid bilayer vesicles by accounting for the effects of spontaneous membrane curvature and radius size. They found that the membrane curvature favored the formation of electric pores. Sadik *et al*. [7] quantified the degree of deformation as a function of the electric-field intensity and the intravesicular-to-extravesicular conductivity ratio under strong dc electric fields. Riske and Dimova [8] used a fast imaging digital camera to observe the deformation and electroporation of giant vesicles exposed to electric pulses. They showed that the shape response of a giant lipid vesicle depended on the membrane properties (e.g., stretching and bending elasticity, surface viscosity, and edge energy) and on the viscosity of the inner and outer electrolytes. Fan and Fedorov [9] studied the interactions between an atomic force microscope tip and a cell membrane by accounting for electrohydrodynamic and surface forces in a dilute electrolyte solution. Hyuga *et al.* proposed a model to describe the static and dynamic deformations of a vesicle in external electric fields, in which the effect of the intravesicular-to-extravesicular conductivity ratio was taken into account [10,11]. It is demonstrated that a vesicle will deform into a prolate shape when the conductivity of the inner medium is higher than that of the outer one.

The deformation behavior of biological cells is dependent on the frequency in the ac electric field. In recognition of the influences of the conductivities of both inner and outer electrolytes on vesicle deformation, Winterhalter and Helfrich conducted a series of studies to determine the deformation of vesicles in an ac electric field by considering the curvature energy and the Maxwell pressure acting on the two interfaces [12]. Based on the Winterhalter-Helfrich model, Peterlin *et al*. [13,14] explained the morphological transition of phospholipid vesicles with respect to the frequency of the ac electric field and the ratio of the conductivities of inner and outer electrolytes. They treated the inner and outer media of the vesicle and the membrane itself as leaky dielectrics and modeled the vesicle as a nearly spherical shell. Considering the asymmetric conductivity conditions across the vesicle membrane in an ac electric field, Yamamoto *et al*. [15] investigated theoretically the stability of spherical vesicles for low, intermediate, and high frequencies. They found that accumulated electric charges could provide the molecular mechanism underlying the vesicle shape transitions. However, these previous works only considered the bending elasticity energy of the membrane and the energy associated with the applied electric field. To date, it remains unclear how factors such as osmotic pressure difference and surface tension contribute to the vesicle deformation in an ac electric field.

It is well known that lipid bilayer membranes exhibit some properties of liquid crystals [16]. Experiments showed that the structure of the lipid bilayers of cell membranes followed the general principles of liquid crystals [17–20]. Tu *et al*. [21–23] successfully applied the elastic theory of liquid-crystal biomembranes based on Helfrich's curvature energy [24] to investigate. Further effort was directed toward understanding the deformation of vesicles in an electric field.

*yliu5@bjtu.edu.cn

Gao *et al*. [25,26] developed a liquid-crystal model for the lipid membrane in electric fields and discussed the morphological evolution of spherical vesicles due to a dc electric field. In the present paper the liquid-crystal model proposed by Gao *et al*. [25,26] is extended to investigate the distinct morphological evolution of vesicles in an ac electric field and to examine the effects of a number of factors, including the Maxwell stresses, elastic bending, osmotic pressure difference, surface tension, and flexoelectric and dielectric properties as well. The layout of this paper is as follows. In Sec. II the governing equations of vesicle morphologies in an ac electric field are derived on the basis of the liquid-crystal vesicle model. In Sec. III this model is used to study the morphological evolution of a spherical vesicle in a wide range of field frequencies. Then the singularity of electric fields in the vesicle is investigated in Sec. IV and several numerical examples are given in Sec. V. The main conclusions drawn from this study will be summarized in Sec. VI.

II. LIQUID-CRYSTAL MODEL FOR VESICLES

In this section the liquid-crystal model of vesicles in a dc electric field [25,26] is briefly reviewed. Then an ac electric field is introduced. In analogy with the curvature elasticity energy of the liquid-crystal model proposed by Helfrich [24], the bending energy of a vesicle can be expressed as

$$F_b = \int_M \left[\frac{1}{2}k(2H + c_0)^2 + k_1 K\right] dA, \tag{1}$$

where M denotes the surface of the vesicle, k and k_1 are its elastic constants, H is the mean curvature, K is the Gauss curvature, and c_0 is the spontaneous curvature. The applied ac electric field is characterized by the angular frequency ω or the field frequency $\nu = \omega/2\pi$. The electric field intensity $\mathbf{E}$ has the general form [15]

$$\mathrm{E} = -\tfrac{1}{2}\nabla\bar{\phi}e^{-i\omega t} + \mathrm{c.c.}, \tag{2}$$

where c.c. stands for complex conjugate, ϕ is the electric potential, and $\bar{\phi}$ denotes the time-independent part of the electric field.

Bending a lipid membrane can induce its electric polarization. This flexoelectric effect results from the orientational strain of polar molecules in the membrane. The flexoelectric energy of a vesicle can be written as

$$F_p = -\int_M \int_0^d \mathbf{P_f}\cdot\mathbf{E}\, dr\, dA, \tag{3}$$

where d is the membrane thickness and $\mathbf{P_f}$ is the bending-induced polarization, which is given by

$$\mathbf{P_f} = -e_1\mathbf{n}(\nabla\cdot\mathbf{n}), \tag{4}$$

where e_1 is the flexoelectric coefficient and $\mathbf{n}$ is the unit vector normal to the membrane surface.

The dielectric energy induced by the electric field can be computed by

$$F_d = -\frac{1}{2}\int_M \int_0^d \mathbf{D}_e\cdot\mathbf{E}\, dr dA, \tag{5}$$

where $\mathbf{D_e}$ is the electric displacement vector. For isotropic constitutive laws, one has

$$\mathbf{D}_e = \varepsilon_2\mathbf{E} = \varepsilon_2(E_n\mathbf{n} + E_u\mathbf{Y}_{,\mathbf{u}} + E_v\mathbf{Y}_{,\mathbf{v}}), \tag{6}$$

where ε_2 is the dielectric constant of the vesicle itself and $\mathbf{Y}_{,u}$ and $\mathbf{Y}_{,v}$ are two tangential vectors of the membrane surface. The normal vector $\mathbf{n}$ and the two vectors $\mathbf{Y}_{,u}$ and $\mathbf{Y}_{,v}$ form a mutually orthogonal local coordinate system on the membrane surface; E_n, E_u, and E_v are the electric-field intensities in the $\mathbf{n}$, $\mathbf{Y}_{,u}$, and $\mathbf{Y}_{,v}$ directions, respectively. The dielectric energy of an electrolyte is written as

$$F_c = -\int \frac{1}{2}\varepsilon_r|\phi|^2 dV, \tag{7}$$

where ε_r denotes the dielectric constant of the electrolyte. Furthermore, the contributions of the osmotic pressure difference $\Delta p = p_{\mathrm{out}} - p_{\mathrm{in}}$ and the surface tension λ to the Helmholtz free energy are given by

$$F_M = \int \Delta p dV + \int_M \lambda dA. \tag{8}$$

From the above equations, the Helmholtz free energy of a vesicle embedded in an electrolyte and subjected to an electric field is expressed as

$$\begin{aligned} F &= F_b + F_p + F_d + F_c + F_M \\ &= \int_M \left(\frac{k(2H + c_0)^2}{2} + \lambda\right) dA + \int \left(\Delta p - \frac{1}{2}\varepsilon_r|\phi|^2\right) dV \\ &\quad - \int_M \int_0^d \left(\mathbf{P_f}\cdot\mathbf{E} + \frac{1}{2}\mathbf{D}_e\cdot\mathbf{E}\right) dr\, dA. \end{aligned} \tag{9}$$

The governing equation of vesicle shape is determined by minimizing the free energy F under the constraints of constant volume V and total area A [27]. The first-order variational of F is

$$\begin{aligned} \delta F &= \delta(F_b + F_p + F_d + F_c + F_M) \\ &= \delta\int_M \left(\frac{k(2H + c_0)^2}{2}\right) dA + \delta\int_M \lambda\, dA \\ &\quad + \delta\left(\int \left(\Delta p - \frac{1}{2}\varepsilon_r|\phi|^2\right) dV\right) \\ &\quad - \delta\left(\int_M \int_0^d (\mathbf{P_f}\cdot\mathbf{E} + \frac{1}{2}\mathbf{D}_e\cdot\mathbf{E}) dr\, dA\right), \end{aligned} \tag{10}$$

where δ denotes the variation with respect to the vesicle shape. From the condition $\delta F = 0$ [25], the shape equation is obtained as

$$\begin{aligned} &\nabla^2(2kH + kc_0) + k(2H + c_0)(2H^2 - c_0 H - 2K) \\ &\quad + \Delta p - 2\lambda H + f = 0, \\ &f = H\int_0^d \varepsilon_2\left(E_n^2 + g_{uu}E_u^2 + g_{vv}E_v^2\right) dr + 2e_1 K\int_0^d E_n dr \\ &\quad - e_1\nabla^2\left(\int_0^d E_n dr\right) + \varepsilon_3\left(E_{3n}^2 - \frac{1}{2}\mathbf{E}_3^2\right) \\ &\quad - \varepsilon_1\left(E_{1n}^2 - \frac{1}{2}\mathbf{E}_1^2\right), \end{aligned} \tag{11}$$

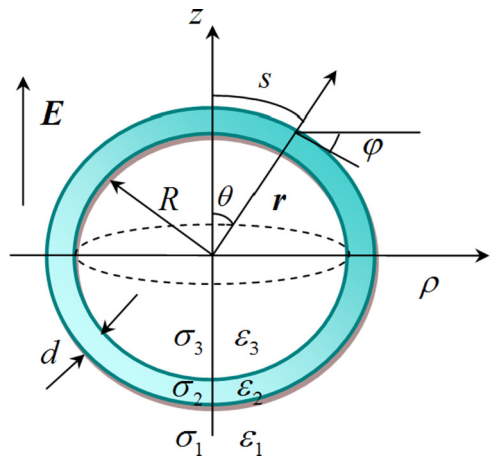

FIG. 1. (Color online) Geometry of an initially spherical vesicle subjected to an ac electric field. The vesicle is denoted by dielectric constant ε_2 and conductivity σ_2.

where ε_3 and ε_1 are the dielectric constants of the inner and outer electrolytes, respectively; $E_{3n} = \mathbf{E}_3 \cdot \mathbf{n}$ and $E_{1n} = \mathbf{E}_1 \cdot \mathbf{n}$ are the normal components of the electric field on the inner and outer surfaces, with $\mathbf{E}_1$ and $\mathbf{E}_3$ being the electric-field intensity of the inner and outer media, respectively; and $g_{uu} = \mathbf{Y}_{,u} \cdot \mathbf{Y}_{,u}$ and $g_{vv} = \mathbf{Y}_{,v} \cdot \mathbf{Y}_{,v}$. In the absence of the electric field $\mathbf{E}$, Eq. (11) returns to the corresponding shape equation for lipid vesicles under purely mechanical forces derived by Ou-Yang and Helfrich [28].

III. SHAPE EQUATIONS FOR AXISYMMETRIC VESICLES IN ac ELECTRIC FIELDS

When subjected to an ac electric field, an axisymmetric vesicle may deform into different forms, e.g., oblate, prolate, and sphere, depending on the field frequency. In this section the general shape equation of vesicles in an ac electric field is formulated based on the liquid-crystal model in Sec. II. It provides an efficient tool to investigate the deformation and stability of a vesicle induced by ac electric and mechanical fields.

A. Axisymmetric vesicles in an ac electric field

Consider an axisymmetric vesicle in an ac electric field, as shown in Fig. 1. To calculate the force induced by the ac electric field, one needs to calculate the electric field around the membrane first. The conductivity of the membrane is very poor. The lipid membrane is essentially an insulating shell impermeable to ions, like leaky dielectrics. When an electric field is applied, charges accumulate on both sides of the bilayer and the membrane acts as a charging capacitor [29]. Since we consider only the case of an applied electric field, the small effects of the induced magnetic field are neglected. Therefore, the electric field can be regarded as irrotational, that is, $\nabla \times \mathbf{E} = \mathbf{0}$. Referring to the usual experimental setup [30], the local charge in the electrolytes is ignored. So we have a restrictive equation for the electric potential [12,15]

$$\nabla^2 \phi_k = 0, \tag{12}$$

with $k = 1, 2, 3$. Here and in the following, the subscripts 1, 2, and 3 stand for the outer medium, the lipid vesicle itself, and the inner medium, respectively. Further, we adopt the isotropic constitutive relation between the electric displacement and the electric-field intensity, that is,

$$\mathbf{D}_k = \varepsilon_k \mathbf{E}_k, \tag{13}$$

with $k = 1,2,3$. The electric potentials and the normal components of the current densities are continuous across the interfaces between the three media. Then the continuity conditions are expressed as

$$\begin{aligned} &\phi_1 = \phi_2, \quad (\sigma_1 - i\omega\varepsilon_1)\nabla\phi_1 \cdot \mathbf{n} = (\sigma_2 - i\omega\varepsilon_2)\nabla\phi_2 \cdot \mathbf{n}, \\ &\phi_2 = \phi_3, \quad (\sigma_2 - i\omega\varepsilon_2)\nabla\phi_2 \cdot \mathbf{n} = (\sigma_3 - i\omega\varepsilon_3)\nabla\phi_3 \cdot \mathbf{n}. \end{aligned} \tag{14}$$

Thus, we can determine the shape of a vesicle in an electric field by solving the nonlinear shape equation (11), in conjunction with the electric-field equation (12) and the boundary conditions (14). However, due to the strong nonlinearity, mechanical and electric coupling effects, and moving boundaries, this problem is generally hard to solve analytically.

B. Shape equation in a spherical coordinate system

Let us take an initially spherical vesicle as an example, as shown in Fig. 1. We refer to the spherical coordinate system and the arc-length coordinate system, where r is the distance from the center of the vesicle, θ is the inclination angle, φ is the angle between the tangent to the contour, ρ is the axis, s is the arc length of the contour, and d is the membrane thickness. The interior and exterior of the vesicle are filled with electrolytes. Their dielectric constants are ε_3 and ε_1 and conductivities are σ_3 and σ_1, respectively.

The Laplace equation (12) can be expressed in terms of the spherical coordinates as

$$\frac{1}{r^2}\frac{\partial}{\partial r}\left(r^2 \frac{\partial \phi}{\partial r}\right) + \frac{1}{r^2 \sin\theta}\frac{\partial}{\partial \theta}\left(\sin\theta \frac{\partial \phi}{\partial \theta}\right) = 0, \tag{15}$$

where $\phi = \phi\,(r,\theta)$. Since the reference equilibrium shape is a sphere, when the perturbations are not large, the solution of Eq. (15) is expected to be of the form [12,15]

$$\phi_k = \frac{1}{2}\left[\left(A_k r + \frac{B_k}{r^2}\right)\cos\theta e^{-i\omega t} + \text{c.c.}\right], \tag{16}$$

where the coefficients A_k and B_k need to be determined from the boundary conditions. In the far field ($r \to \infty$), the electric potential is unperturbed by the presence of the vesicle, whereas at the center of the vesicle ($r = 0$), the potential has a finite value. From these two conditions, one can immediately obtain

$$A_1 = -E_0, \quad B_3 = 0. \tag{17}$$

Then the electric potentials are derived as

$$\begin{aligned} \phi_1 &= \frac{1}{2}\left[\left(-E_0 r + \frac{B_1}{r^2}\right)\cos\theta e^{-i\omega t} + \text{c.c.}\right], \\ \phi_2 &= \frac{1}{2}\left[\left(A_2 r + \frac{B_2}{r^2}\right)\cos\theta e^{-i\omega t} + \text{c.c.}\right], \\ \phi_3 &= \frac{1}{2}(A_3 r \cos\theta e^{-i\omega t} + \text{c.c.}). \end{aligned} \tag{18}$$

We define $r = l(\theta)$, with l the distance of the vesicle center to the inner membrane. Then the four boundary conditions in Eq. (14) are rewritten as

$$\frac{B_1}{(l+d)^2} - E_0(l+d) = A_2(l+d) + \frac{B_2}{(l+d)^2}, \tag{19}$$

$$A_2 l + \frac{B_2}{l^2} = A_3 l, \tag{20}$$

$$A_3\left(l\cos\theta + \frac{dl}{d\theta}\sin\theta\right) = \beta_3\left[A_2\left(l\cos\theta + \frac{dl}{d\theta}\sin\theta\right) - \frac{B_2}{l^3}\left(2l\cos\theta - \frac{dl}{d\theta}\sin\theta\right)\right], \tag{21}$$

$$\left[A_2\left(l\cos\theta + \frac{dl}{d\theta}\sin\theta\right) - \frac{B_2}{(l+d)^3}\left(2l\cos\theta - \frac{dl}{d\theta}\sin\theta\right)\right] = \beta_1\left[-E_0\left(l\cos\theta + \frac{dl}{d\theta}\sin\theta\right) - \frac{B_1}{(l+d)^3}\left(2l\cos\theta - \frac{dl}{d\theta}\sin\theta\right)\right], \tag{22}$$

where

$$\beta_1 = \frac{\sigma_2 - i\omega\varepsilon_2}{\sigma_1 - i\omega\varepsilon_1}, \tag{23}$$

$$\beta_3 = \frac{\sigma_2 - i\omega\varepsilon_2}{\sigma_3 - i\omega\varepsilon_3}. \tag{24}$$

In the derivation of Eqs. (21) and (22), the normal unit vector $\mathbf{n}$ of the generator for the axisymmetric surface has been used, which is expressed as

$$\mathbf{n} = \left[\frac{-(dl/d\theta)\cos\theta + l\sin\theta}{\sqrt{(dl/d\theta)^2 + l^2}}, \frac{(dl/d\theta)\sin\theta + l\cos\theta}{\sqrt{(dl/d\theta)^2 + l^2}}\right]^{\mathrm{T}}. \tag{25}$$

The four coefficients A_2, A_3, B_1, and B_2 can be determined from Eqs. (19)–(22) and are given in Appendix A.

In the special case of a spherical vesicle ($dl/d\theta = 0$), the coefficients reduce to

$$A_2 = -\frac{3E_0(1+2\beta)}{(1+2\beta)(2+\beta) - 2\gamma^3(1-\beta)^2}, \tag{26}$$

$$A_3 = -\frac{9E_0\beta}{(1+2\beta)(2+\beta) - 2\gamma^3(1-\beta)^2}, \tag{27}$$

$$B_1 = E_0(R+d)^3 - \frac{3E_0(R+d)^3[(1+2\beta) - \gamma^3(1-\beta)]}{(1+2\beta)(2+\beta) - 2\gamma^3(1-\beta)^2}, \tag{28}$$

$$B_2 = \frac{3E_0R^3(1-\beta)}{(1+2\beta)(2+\beta) - 2\gamma^3(1-\beta)^2}, \tag{29}$$

where R is the inner radius of the vesicle. When the dimensionless parameters β and γ are defined, respectively, as [12]

$$\beta = \beta_1 = \beta_3 = \frac{\sigma_2 - i\omega\varepsilon_2}{\sigma_1 - i\omega\varepsilon_1} = \frac{\sigma_2 - i\omega\varepsilon_2}{\sigma_3 - i\omega\varepsilon_3}, \tag{30}$$

$$\gamma = \frac{R}{R+d}, \tag{31}$$

the coefficients in Eqs. (26)–(29) are consistent with those derived by Winterhalter and Helfrich [12].

The stable shape of the vesicle is determined by the Maxwell stresses, dielectric energy density, the ratio $\chi = d/l$, and β_1 and β_3. In general, the membrane thickness d is much smaller than l; β_1 and β_3 are also small quantities because the conductivity of the membrane is much lower than those of the internal and external medium and the permittivity of the membrane is one order of magnitude smaller than those of the internal and external ones. A simplification is possible when the above conditions are taken into account. In those cases, the asymptotic expression of the terms in the shape equation associated with the electric field can be derived as

$$E_{\mathrm{int}2} = \int_0^d E_n dr = \frac{3}{2}\chi E_0 l^3\cos^2\theta\left(l\cos\theta + \frac{dl}{d\theta}\sin\theta\right) \times\left[\frac{e^{-i\omega t}}{a_1+a_2} + \frac{e^{i\omega t}}{(a_1+a_2)^*}\right]\left[\left(\frac{dl}{d\theta}\right)^2 + l^2\right]^{-1/2}, \tag{32}$$

$$U_2 = \varepsilon_2\int_0^d \left(E_n^2 + E_u^2 + E_v^2\right)dr = \frac{9}{4}\varepsilon_2\chi E_0^2 l^3\cos^4\theta\left(l\cos\theta + \frac{dl}{d\theta}\sin\theta\right)^2 \times\left[\frac{e^{-i\omega t}}{a_1+a_2} + \frac{e^{i\omega t}}{(a_1+a_2)^*}\right]^2, \tag{33}$$

$$f_3 = \varepsilon_3\left(E_{3n}^2 - \frac{1}{2}E_3^2\right) = \frac{1}{8}\varepsilon_3\left[l^2\cos 2\theta - \left(\frac{dl}{d\theta}\right)^2\cos 2\theta + 2l\frac{dl}{d\theta}\sin 2\theta\right] \times(Ae^{-i\omega t} + A^*e^{i\omega t})^2\left[\left(\frac{dl}{d\theta}\right)^2 + l^2\right]^{-1}, \tag{34}$$

$$f_1 = \varepsilon_1\left(E_{1n}^2 - \frac{1}{2}E_1^2\right) = \frac{1}{8}\varepsilon_1[(Be^{-i\omega t} + B^*e^{i\omega t})^2 - (Ce^{-i\omega t} + C^*e^{i\omega t})^2]\left[\left(\frac{dl}{d\theta}\right)^2 + l^2\right]^{-1}, \tag{35}$$

where

$$a_1 = \chi\left(2l\cos\theta - \frac{dl}{d\theta}\sin\theta\right)\left(l\cos\theta + \frac{dl}{d\theta}\sin\theta\right), \tag{36}$$

$$a_2 = l\cos\theta\left[\beta_3\left(2l\cos\theta - \frac{dl}{d\theta}\sin\theta\right) + \beta_1\left(l\cos\theta + \frac{dl}{d\theta}\sin\theta\right)\right], \tag{37}$$

$$A = \frac{3\beta_3 E_0 l^2 \cos^2\theta}{a_1 + a_2}, \tag{38}$$

$$B = \frac{3\beta_1 E_0 l^2 \cos^2\theta \left(l\cos\theta + \frac{dl}{d\theta}\sin\theta\right)}{a_1 + a_2}, \tag{39}$$

$$C = \frac{3E_0\left[\beta_1 \frac{dl}{d\theta} l \cos^2\theta \left(l\cos\theta + \frac{dl}{d\theta}\sin\theta\right)\right]}{a_1 + a_2} - \frac{3E_0 \sin\theta\cos\theta\left[\left(\frac{dl}{d\theta}\right)^2 + l^2\right]}{a_1 + a_2} \times \left[\chi\left(l\cos\theta + \frac{dl}{d\theta}\sin\theta\right) + \beta_3 l\cos\theta\right]. \tag{40}$$

The asterisk stands for a complex conjugate, E_{int2} is the transmembrane voltage drop, U_2 is the dielectric energy density, and f_1 and f_3 are the Maxwell pressures of the inner and outer interfaces, respectively.

To derive the shape equation of a vesicle at the steady state, we average the trans-membrane voltage drop, the Maxwell stresses, and the dielectric energy density over a period of the ac electric field [15,30]. The corresponding electric parts are rewritten as

$$\bar{E}_{\text{int2}} \equiv \langle E_{\text{int2}} \rangle = 0, \tag{41}$$

$$\bar{U}_2 \equiv \langle U_2 \rangle = \frac{9\varepsilon_2 \chi E_0^2 l^3 \cos^4\theta (l\cos\theta + \frac{dl}{d\theta}\sin\theta)^2}{2(a_1 + a_2)(a_1 + a_2)^*}, \tag{42}$$

$$\bar{f}_3 \equiv \langle f_3 \rangle = \frac{AA^*}{4}\varepsilon_3 \left[l^2\cos 2\theta - \left(\frac{dl}{d\theta}\right)^2 \cos 2\theta + 2l\frac{dl}{d\theta}\sin 2\right]\left[\left(\frac{dl}{d\theta}\right)^2 + l^2\right]^{-1}, \tag{43}$$

$$\bar{f}_1 \equiv \langle f_1 \rangle = \frac{1}{4}\varepsilon_1 (BB^* - CC^*)\left[\left(\frac{dl}{d\theta}\right)^2 + l^2\right]^{-1}, \tag{44}$$

where $\langle x \rangle$ stands for the time average of x over a period of the ac electric field.

In the spherical coordinate system, the mean curvature H, the Gaussian K, and the Laplace-Beltrami operator of H can be easily obtained as [25]

$$K = \frac{\left[l\sin\theta - \frac{dl}{d\theta}\cos\theta\right]\left[2\left(\frac{dl}{d\theta}\right)^2 - l\frac{d^2l}{d\theta^2} + l^2\right]}{l\sin\theta\left[\left(\frac{dl}{d\theta}\right)^2 + l^2\right]^2}, \tag{45}$$

$$H = \frac{\cos\theta\left[l^2\left(\frac{dl}{d\theta}\right) + \left(\frac{dl}{d\theta}\right)^3\right]}{2l\sin\theta\left[\left(\frac{dl}{d\theta}\right)^2 + l^2\right]^{3/2}} - \frac{\sin\theta\left[2l^3 - l^2\left(\frac{d^2l}{d\theta^2}\right) + 3l\left(\frac{dl}{d\theta}\right)^2\right]}{2l\sin\theta\left[\left(\frac{dl}{d\theta}\right)^2 + l^2\right]^{3/2}}, \tag{46}$$

$$\nabla^2 H = \frac{D_4\left(\frac{d^4l}{d\theta^4}\right) + D_3\left(\frac{d^3l}{d\theta^3}\right) + D_{23}\left(\frac{d^2l}{d\theta^2}\right)^3}{2l^3\sin^3\theta\left[\left(\frac{dl}{d\theta}\right)^2 + l^2\right]^{9/2}} + \frac{D_{22}\left(\frac{d^2l}{d\theta^2}\right)^2 + D_{21}\left(\frac{d^2l}{d\theta^2}\right) + D_1}{2l^3\sin^3\theta\left[\left(\frac{dl}{d\theta}\right)^2 + l^2\right]^{9/2}}. \tag{47}$$

The coefficients D_1, D_{21}, D_{22}, D_{23}, D_3, and D_4 are given in Appendix B.

Substitution of Eqs. (41)–(47) into (11) yields the electroelastic shape equation of vesicles in ac electric field

$$2\nabla^2 H + (2H + c_0)(2H^2 - c_0 H - 2K) + \frac{1}{k}(\Delta p - 2\lambda H + H\bar{U}_2 + \bar{f}_3 - \bar{f}_1) = 0. \tag{48}$$

For a spherical vesicle with radius R, we have

$$K = \frac{1}{R^2}, \quad H = -\frac{1}{R}, \quad \nabla^2 H = 0 \tag{49}$$

and Eq. (11) is recast as

$$\Delta p + \frac{2\lambda}{R} + kc_0\left(\frac{c_0}{R} - \frac{2}{R^2}\right) - \frac{9\varepsilon_2 E_0^2 d\cos^2\theta}{2R(2d/R + 2\beta_3 + \beta_1)(2d/R + 2\beta_3 + \beta_1)^*} + \frac{9\varepsilon_3\beta_3\beta_3^* E_0^2\cos 2\theta}{4(2d/R + 2\beta_3 + \beta_1)(2d/R + 2\beta_3 + \beta_1)^*} - \frac{9\varepsilon_1\beta_1\beta_1^* E_0^2\cos^2\theta}{4(2d/R + 2\beta_3 + \beta_1)(2d/R + 2\beta_3 + \beta_1)^*} + \frac{9\varepsilon_1 E_0^2\sin^2\theta(d/R + \beta_3)(d/R + \beta_3)^*}{4(2d/R + 2\beta_3 + \beta_1)(2d/R + 2\beta_3 + \beta_1)^*} = 0. \tag{50}$$

Generally, a vesicle maintains a spherical shape in an ac electric field when Eq. (50) has a nontrivial solution independent of the angular coordinate. Obviously, Eq. (50) should satisfy the condition

$$\Delta p + \frac{2\lambda}{R} + kc_0\left(\frac{c_0}{R} - \frac{2}{R^2}\right) + \frac{9\varepsilon_1 E_0^2(d/R + \beta_3)(d/R + \beta_3)^* - 9\varepsilon_3\beta_3\beta_3^* E_0^2}{4(2d/R + 2\beta_3 + \beta_1)(2d/R + 2\beta_3 + \beta_1)^*} = 0, \tag{51}$$

$$2\varepsilon_3\beta_3\beta_3^* - \varepsilon_1\beta_1\beta_1^* - \varepsilon_1\left(\frac{d}{R} + \beta_3\right)\left(\frac{d}{R} + \beta_3\right)^* - \frac{2\varepsilon_2 d}{R} = 0. \tag{52}$$

It can be seen that the stability of spherical morphology of the vesicle under an ac electric field depends on the frequency, the pressure difference, the surface tension, the dielectric coefficient of the membrane, the thickness of the membrane, and the conductivities of the inner and outer electrolytes.

C. Shape equation in terms of axisymmetric and arc-length coordinates

In the axisymmetric coordinate system (ρ,φ) in Fig. 1, the mean curvature H, Gaussian curvature K, and the Laplace-Beltrami operator of H have the form

$$K = \frac{\sin\varphi\cos\varphi}{\rho}\frac{d\varphi}{d\rho}, \tag{53}$$

$$H = -\frac{\cos\varphi}{2}\frac{d\varphi}{d\rho} - \frac{\sin\varphi}{2\rho}, \tag{54}$$

$$\nabla^2 H = -\frac{1}{2\rho^3}\left\{\rho^2\cos^3\varphi\left(\rho\frac{d^3\varphi}{d\rho^3}+2\frac{d^2\varphi}{d\rho^2}\right)-\sin\varphi\cos^2\varphi\left[3\rho^2\left(\frac{d\varphi}{d\rho}\right)^2+4\rho^3\frac{d\varphi}{d\rho}\frac{d^2\varphi}{d\rho^2}-1\right]\right.$$
$$\left.-\rho\cos 2\varphi\cos\varphi\left[\rho^2\left(\frac{d\varphi}{d\rho}\right)^3+\frac{d\varphi}{d\rho}\right]\right\}. \tag{55}$$

The electric field has the relations

$$E_{\text{int}21} = \int_0^d E_n dr = \frac{3}{2}E_0 z^2(z\cos\varphi+\rho\sin\varphi)\sqrt{\rho^2+z^2}\cos\varphi\left[\frac{e^{-i\omega t}}{a_3+a_4}+\frac{e^{i\omega t}}{(a_3+a_4)^*}\right], \tag{56}$$

$$U_{21} = \varepsilon_2\int_0^d\left(E_n^2+E_u^2+E_v^2\right)dr = \frac{9\varepsilon_2 E_0^2 z^4(\rho^2+z^2)^2\cos^2\varphi}{4d}\left[\frac{e^{-i\omega t}}{a_3+a_4}+\frac{e^{i\omega t}}{(a_3+a_4)^*}\right]^2, \tag{57}$$

$$f_{31} = \varepsilon_3\left(E_{3n}^2-\tfrac{1}{2}E_3^2\right) = \tfrac{9}{8}\varepsilon_3 E_0^2 z^4(De^{-i\omega t}+D^*e^{i\omega t})^2\cos 2\varphi, \tag{58}$$

$$f_{11} = \varepsilon_1\left(E_{1n}^2-\tfrac{1}{2}E_1^2\right) = \tfrac{1}{8}\varepsilon_1[(Fe^{-i\omega t}+F^*e^{i\omega t})^2-(Ge^{-i\omega t}+G^*e^{i\omega t})^2], \tag{59}$$

where

$$a_3 = \frac{[3\rho z\sin\varphi+(2z^2-\rho^2)\cos\varphi](\rho^2+z^2)\cos\varphi}{z\cos\varphi+\rho\sin\varphi}, \tag{60}$$

$$a_4 = \frac{z(z\cos\varphi+\rho\sin\varphi)}{d}\{\beta_1(\rho^2+z^2)\cos\varphi+\beta_3[3\rho z\sin\varphi+(2z^2-\rho^2)\cos\varphi]\}, \tag{61}$$

$$D = \frac{\beta_3(z\cos\varphi+\rho\sin\varphi)^2}{d(a_3+a_4)}, \tag{62}$$

$$F = \frac{3\beta_1 E_0 z^2\cos\varphi(z\cos\varphi+\rho\sin\varphi)^2}{d(a_3+a_4)}, \tag{63}$$

$$G = \frac{3E_0(z\cos\varphi+\rho\sin\varphi)[\beta_1 z^2\cos\varphi(\rho\cos\varphi-z\sin\varphi)-\beta_3\rho z^2]}{d(a_3+a_4)}-\frac{3E_0\rho z(\rho^2+z^2)\cos\varphi}{(a_3+a_4)(z\cos\varphi+\rho\sin\varphi)}. \tag{64}$$

At the steady state of the vesicle, the time average of the Maxwell stresses, the trans-membrane voltage drop, and the dielectric energy density over a period of ac electric field are

$$\bar{E}_{\text{int}21} \equiv \langle E_{\text{int}21}\rangle = 0, \tag{65}$$

$$\bar{U}_{21} \equiv \langle U_{21}\rangle = \frac{9\varepsilon_2 E_0^2 z^4(\rho^2+z^2)^2\cos^2\varphi}{2d(a_3+a_4)(a_3+a_4)^*}, \tag{66}$$

$$\bar{f}_{31} \equiv \langle f_{31}\rangle = \frac{9}{4}\varepsilon_3 E_0^2 z^2 DD^*\cos 2\varphi, \tag{67}$$

$$\bar{f}_{11} \equiv \langle f_{11}\rangle = \frac{1}{4}\varepsilon_1(FF^*-GG^*). \tag{68}$$

Inserting Eqs. (53)–(59) into Eq. (11), the electroelastic shape equation for a vesicle in the axisymmetric coordinate system is determined as

$$2\nabla^2 H+(2H+c_0)(2H^2-c_0H-2K)$$
$$+\frac{1}{k}(\Delta p-2\lambda H+H\bar{U}_{21}+\bar{f}_{31}-\bar{f}_{11}) = 0. \tag{69}$$

If $\omega = 0$ and $E_0 = 0$, the shape equation reduces to

$$\cos^3\varphi\ddot{\varphi}-4\sin\varphi\cos^2\varphi\ddot{\varphi}\dot{\varphi}+\cos\varphi\left(1-\frac{3\cos^2\varphi}{2}\right)\dot{\varphi}^3$$
$$-\frac{7\sin\varphi\cos^2\varphi}{2\rho}\dot{\varphi}^2+\frac{2\cos^3\varphi\ddot{\varphi}}{\rho}-\frac{\Delta p}{k}-\frac{\lambda\sin\varphi}{k\rho}$$
$$-\cos\varphi\left(\frac{c_0^2}{2}-\frac{2c_0\sin\varphi}{\rho}+\frac{3\cos^2\varphi-1}{2\rho^2}+\frac{\lambda}{k}\right)\dot{\varphi}$$
$$+\frac{\sin^2\varphi}{2\rho^3}-\frac{c_0^2\sin\varphi}{2\rho}+\frac{\sin\varphi\cos^2\varphi}{\rho^3} = 0, \tag{70}$$

where the overdot represents the derivation with respect to ρ. Equation (70) is consistent with the shape equation derived by Hu and Ou-Yang [27] for vesicles in mechanical fields.

Similarly, in the arc-length coordinate system, the mean curvature H, the Gaussian curvature K, and the

Laplace-Beltrami operator of H are obtained as

$$K = \frac{\sin\varphi}{\rho}\frac{d\varphi}{ds}, \tag{71}$$

$$H = -\frac{1}{2}\frac{d\varphi}{ds} - \frac{\sin\varphi}{2\rho}, \tag{72}$$

$$\nabla^2 H = \frac{\sin\varphi}{2\rho}\left(\frac{d\varphi}{ds}\right)^2 + \frac{\cos 2\varphi}{2\rho^2}\frac{d\varphi}{ds} - \left(\frac{\sin\varphi\cos^2\varphi}{2\rho^3} + \frac{1}{2}\frac{d^3\varphi}{ds^3} + \frac{\cos\varphi}{\rho}\frac{d^2\varphi}{ds^2}\right). \tag{73}$$

Then the shape equation for vesicles in the arc-length coordinate system is written as

$$2\nabla^2 H + (2H + c_0)(2H^2 - c_0 H - 2K) + \frac{1}{k}(\Delta p - 2\lambda H + H\bar{U}_{22} + \bar{f}_{32} - \bar{f}_{12}) = 0. \tag{74}$$

The expressions of $\bar{U}_{22}$, $\bar{f}_{32}$, and $\bar{f}_{12}$ in terms of the arc-length coordinates are the same as $\bar{U}_{21}$, $\bar{f}_{31}$, and $\bar{f}_{11}$ in Eqs. (65)–(68), except that the variables z and ρ are functions of arc length s. If $\omega = 0$ and $E_0 = 0$, the shape equation (74) reduces to that given by Ou-Yang *et al.* [31] for vesicles in mechanical fields, that is,

$$\varphi''' + \frac{2\cos\varphi\varphi''}{\rho} + \frac{1}{2}\varphi'^3 - \frac{3\sin\varphi\varphi'^2}{2\rho} - \left[\frac{c_0^2}{2} + \frac{\lambda}{k} - \frac{2c_0\sin\varphi}{\rho} + \frac{3\cos^2\varphi - 1}{2\rho^2}\right]\varphi' - \frac{c_0^2\sin\varphi}{2\rho} + \frac{\sin\varphi(1+\cos^2\varphi)}{2\rho^3} - \frac{\Delta p}{k} = 0, \tag{75}$$

where the prime represents the derivative with respect to s.

IV. SINGULARITY OF ac ELECTRIC FIELDS

It is known that an applied electric field can lead to electroporation in cell membranes and a considerable increase in the membrane permeability to ions, molecules, and even macromolecules [31]. Gao *et al.* [25] revealed the electric singularity on the vesicle under a dc electric field. In the present paper the singularity induced by an ac electric field is investigated based on the shape equation given above.

From Eqs. (65)–(68), when $a_3 + a_4 = 0$, the dielectric energy and the Maxwell stresses will become infinite. Then we have

$$\Delta f = \frac{[3\rho z\sin\varphi + (2z^2 - \rho^2)\cos\varphi](\rho^2 + z^2)\cos\varphi}{z\cos\varphi + \rho\sin\varphi} + \frac{z(z\cos\varphi + \rho\sin\varphi)}{d}\{\beta_3[3\rho z\sin\varphi + (2z^2 - \rho^2)\cos\varphi]\} + \frac{z(z\cos\varphi + \rho\sin\varphi)}{d}[\beta_1(\rho^2 + z^2)\cos\varphi] = 0. \tag{76}$$

In contrast to the case of a dc electric field, the singularity of dielectric energy and the Maxwell stress are frequency dependent. In addition, the singularity of an ac electric field is also influenced by the local curvature, electrolyte conductivity, and electrolyte permittivity. From Eq. (76) one can determine the positions at which the electric field is singular and may cause the formation of small pores.

The electric singularity on a vesicle subjected to an ac electric field helps us to understand the formation of electroporation. For red blood cell membranes exposed to an applied electric field, highly concentrated deformation can be observed at some positions [32,33]. In Sec. V a numerical example of a biconcave vesicle in an electric field with different frequencies will be provided to further discuss the electric singularity.

V. EXAMPLES AND DISCUSSION

A. Deformation of vesicles

As mentioned above, the vesicle shape in an ac electric field is frequency dependent. On the basis of the shape equation obtained above, four numerical examples based on Eq. (69) are given to simulate the shape evolution of vesicles in an axisymmetric ac electric field with a frequency in the range from 30×10^3 to 4×10^6 Hz. Besides the frequency dependence, the effects of the pressure difference and surface tension on the shape evolution are also examined. In this situation, Eq. (69) is rewritten as a set of ordinary differential equations in the arc-length coordinate

$$\dot{\varphi} = W, \quad \dot{W} = \tau, \quad \dot{\tau} = F(\varphi,\rho,z,W,\tau), \quad \dot{\rho} = \cos\varphi, \quad \dot{z} = -\sin\varphi, \tag{77}$$

where

$$F(\varphi,\rho,z,W,\tau) = -\frac{2\cos\varphi\ddot{\varphi}}{\rho} - \frac{1}{2}\dot{\varphi}^3 + \left(\frac{1}{2}c_0^2 + \frac{\lambda}{k} + \frac{3\cos^2\varphi - 1}{2\rho^2}\right)\dot{\varphi} + \frac{1}{k}(\Delta p + H\bar{U}_{22} + \bar{f}_{32} - \bar{f}_{12}) + \frac{\sin\varphi}{2\rho^3}\left[\rho^2\left(3\dot{\varphi}^2 - 4c_0 + c_0^2\right) - (1+\cos\varphi)^2\right]. \tag{78}$$

Considering the symmetry of the problem, the boundary conditions for a quadrant of geometry are

$$\varphi(0) = 0, \quad \varphi(s_1) = \frac{\pi}{2}, \quad W(0) = 0, \quad \tau(0) = 0, \quad \rho(0) = 0, \quad \rho(s_1) = \frac{\pi}{2}, \quad z(0) = z_1, \tag{79}$$

where s_1 is the arc length of the integration interval and z_1 is the assumed initial value of $z(0)$. Moreover, the vesicle volume of V_0 is fixed as a constant, that is,

$$\int_0^{s_1} \pi\rho^2\sin\varphi ds = V_0. \tag{80}$$

To explore the deformation features of vesicles, we simulate the equilibrium shapes of a vesicle under different frequencies of the applied ac electric field, as shown in Fig. 2. The parameters used in our calculations are listed in Table I.

A series of meridian planes in the (ρ_1, ρ_2, z) space are chosen, each of which corresponds to a specified frequency. From the (ρ_1, 0, z) plane to the (0, ρ_2, z) plane, the frequency increases from 30 kHz to 4 MHz. It can be seen that the shapes

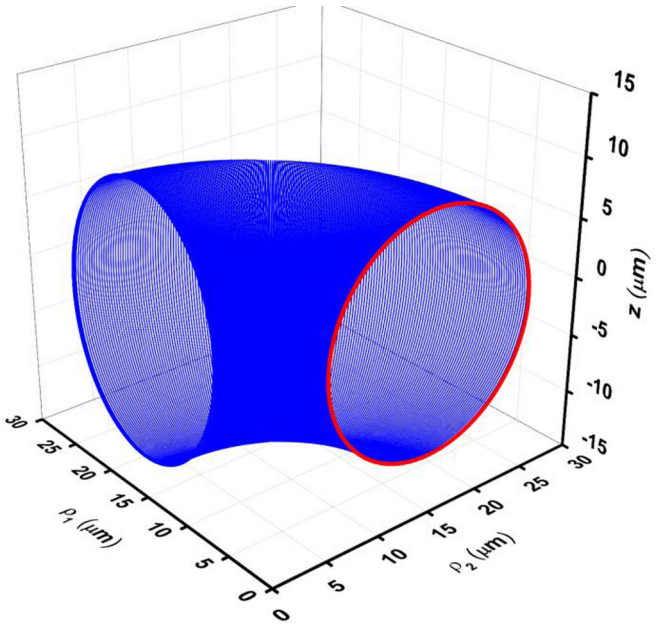

FIG. 2. (Color online) Shape transition of a vesicle with respect to the variation of the frequency, where we set $\sigma_3/\sigma_1 = 4.64$. Each meridian plane represents a specified frequency. From the (ρ_1, 0, z) plane to the (0, ρ_2, z) plane, the frequency increases from 30 kHz to 4 MHz.

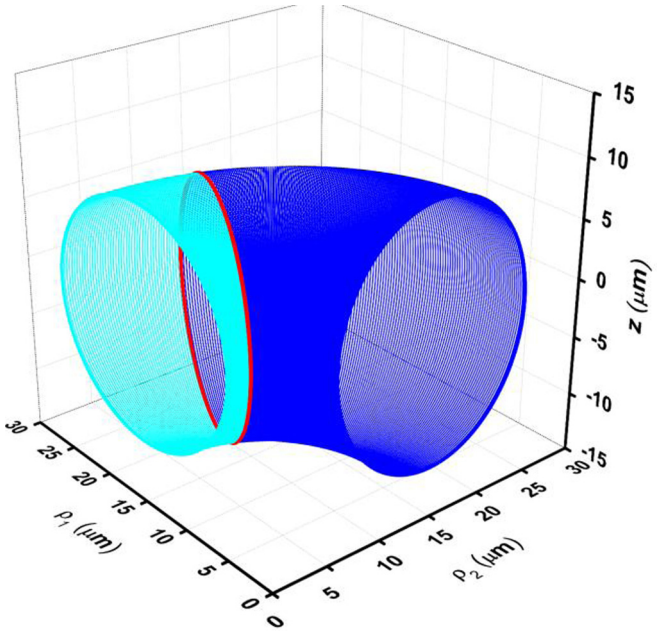

FIG. 3. (Color online) Shape transition of a vesicle with respect to the variation of the osmotic pressure difference Δp, where we set $\sigma_3/\sigma_1 = 4.64$ and $\nu = 4$ MHz. Every meridian plane represents a specified pressure difference. From the (ρ_1, 0, z) plane to the (0, ρ_2, z) plane, the pressure difference increases from -5.6×10^{-6} to -2×10^{-4} Pa.

of vesicles in an ac electric field are frequency dependent. At a relatively low frequency, e.g., $\nu = 30$ kHz, the vesicle has a prolate shape with the major axis along the z direction. With the increase of the frequency, the major axis gradually shortens while the minor axis elongates. The vesicle will have a spherical shape at a high frequency, e.g., $\nu = 4$ MHz (the red solid curve in Fig. 2). These results are in good agreement with the experimental observations of Aranda *et al.* [1] and Yamamoto *et al.* [15].

To illustrate the influence of the osmotic pressure difference, Fig. 3 shows the shape evolution of a vesicle with respect to the variation of the pressure difference. Every meridian plane in the (ρ_1, ρ_2, z) space represents a specified osmotic pressure difference. From the (ρ_1, 0, z) plane to the (0, ρ_2, z) plane, the osmotic pressure difference increases from -5.6×10^{-6} to -2×10^{-4} Pa. The parameters used in the calculations are listed in Table I. We take the electric-field frequency $\nu = 4$ MHz and $\sigma_3/\sigma_1 = 4.64$. If the vesicle shape was independent of the osmotic pressure difference, the vesicle form would be a sphere, as shown by the red solid curve at $\Delta p = -5.6 \times 10^{-5}$ Pa in Fig. 2. However, it can be seen clearly from Fig. 3 that with the increase of the osmotic pressure difference, the vesicle shape changes from an oblate one with the minor axis along the z direction (cyan solid curve) to a sphere at $\Delta p = -5.6 \times 10^{-5}$ Pa (red solid line). As the pressure difference is increased further, the vesicle will become a prolate shape with the major axis along the z direction. Therefore, the pressure difference has a distinct influence on the vesicle morphology. Under a larger pressure difference, the equilibrium shapes of vesicles tend to be prolate. Increasing the pressure difference promotes the critical frequency for the vesicle morphology evolution from a prolate shape to a sphere.

TABLE I. Values of parameters taken in the calculations.

Parameter	Value
cell radius R	1×10^{-5} m
membrane thickness d	5×10^{-9} m
curvature stiffness k	1×10^{-19} J
flexoelectric effect coefficient e_{11}	0 C/m
conductivity of outer medium σ_1	215.5 mS/m
conductivity of inner medium σ_3	1000 mS/m
conductivity of cell membrane σ_2	3×10^{-4} mS/m
permittivity of inner cytoplasm ε_3	6.4×10^{-10} A s/V m
permittivity of cell membrane ε_2	1.6×10^{-11} A s/V m
permittivity of extracellular medium ε_1	6.4×10^{-10} A s/V m
spontaneous curvature c_0	-2.4×10^{-5} m^{-1}
osmotic pressure difference Δp	-5.6×10^{-5} Pa
surface tension λ	-5×10^{-9} N/m
magnitude of electric field E_0	0.1 kV/m

The influence of surface tension λ on the shape evolution of a vesicle in an ac field is shown in Fig. 4, in which the parameters in Table I are used. Each sectional plane in the (ρ_1, ρ_2, z) space corresponds to a given surface tension. In Fig. 4(a), 180 meridian planes are chosen from the (0, ρ_2, z) plane to the (ρ_1, 0, z) plane, with the surface tension varying from -5.6×10^{-9} to -4×10^{-9} N/m. It is found that the vesicle form also shows a dependence on the values of the surface tension. When the value of surface tension λ is small (e.g., -4×10^{-9} N/m), the vesicle takes an oblate shape with the minor axis along the z direction, as shown by the cyan solid curve in Fig. 4(a), where we set $\nu = 4$ MHz and $\sigma_3/\sigma_1 = 4.64$. For a higher surface tension (e.g., 5.6×10^{-9} N/m), the vesicle will have a prolate shape with the major axis along the z direction, as shown by the blue solid curve in

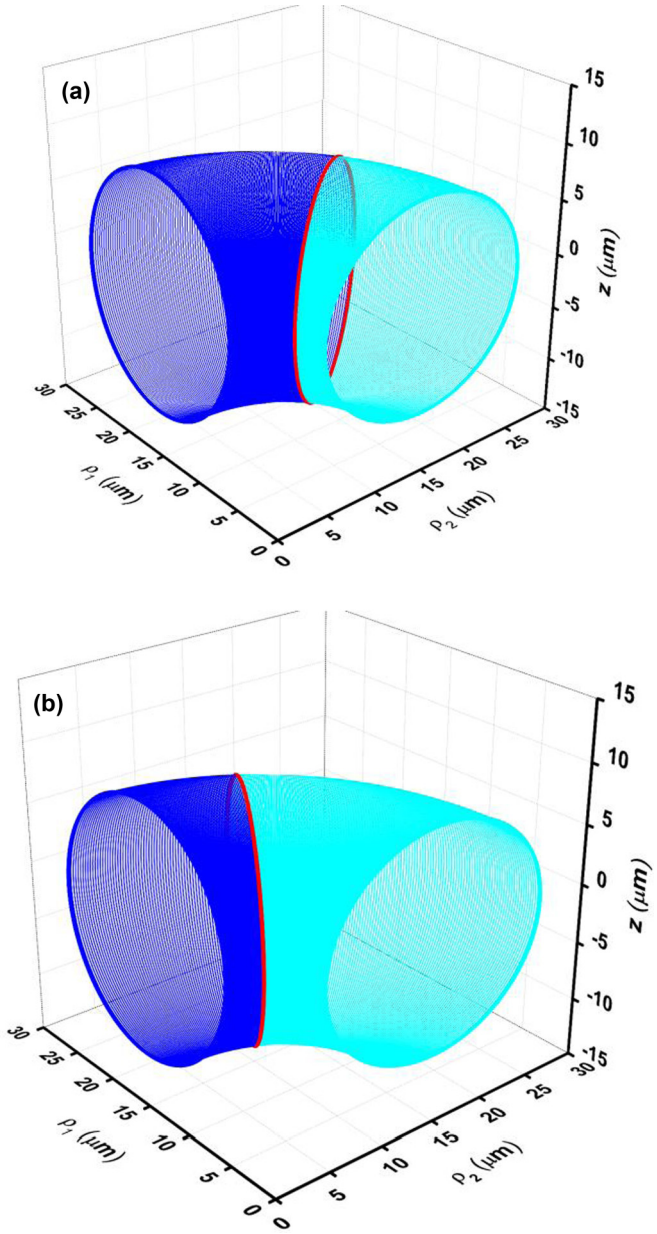

FIG. 4. (Color online) Shape transition of a vesicle with respect to the variation of the surface tension λ when $\sigma_3/\sigma_1 = 4.64$. Every meridian plane in the (ρ_1, ρ_2, z) space represents a specified surface tension. From the $(0, \rho_2, z)$ plane to the $(\rho_1, 0, z)$ plane, the values of the surface tension are increased gradually: (a) $\nu = 4$ MHz, the surface tension varies from -5.6×10^{-9} to -4×10^{-9} N/m; (b) $\nu = 1.5$ MHz, the surface tension varies from -5×10^{-9} to -3.8×10^{-9} N/m.

Fig. 4(a). Figure 4(b) shows the shape evolution of a vesicle with respect to the surface tension λ when $\nu = 1.5$ MHz and $\sigma_3/\sigma_1 = 4.64$. The surface tension varies from -5×10^{-9} to -3.8×10^{-9} N/m. With a decrease of the surface tension, the vesicle morphology undergoes a prolate-sphere-oblate transition, indicating the significant role of surface tension. A comparison between Figs. 4(a) and 4(b) indicates that along with the increase of the electric-field frequency, the critical value corresponding to the prolate-sphere transition due to the variation of the surface tension is decreased.

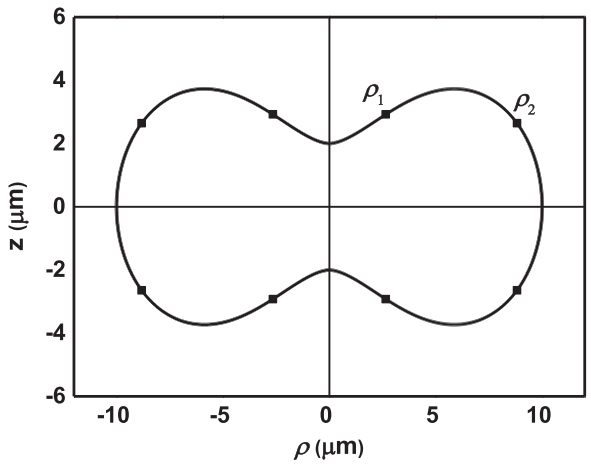

FIG. 5. Vesicle of circular biconcave shape subjected to an ac electric field along the z direction. The square stands for the positions fulfilling the singularity condition given by Eq. (76).

B. Singularity of ac electric fields

Now we analyze the singularity of ac electric fields on the vesicle surface. Following Gao *et al.* [25], a biconcave vesicle is considered. Since the biconcave liposomes begin to deform with increasing osmotic pressure difference, it is reasonable to assume that the initial biconcave vesicles exist at $\Delta p = 0$ and $\lambda = 0$ [34]. The biconcave shape equation of the vesicle is assumed to be [34]

$$\sin\varphi = \rho/R_0 + c_0\rho\ln\rho, \tag{81}$$

where R_0 is the arbitrary constant and c_0 the spontaneous curvature of the membrane. A typical and stationary shape of vesicle is shown in Fig. 5, where we set

$$\sin\varphi = 0.1\rho + 0.188\rho\ln 0.1\rho, \quad \rho \in [0,10]. \tag{82}$$

Let us assume that an ac electric field of intensity $E_0 = 0.1$ kV/m is suddenly applied on the circular biconcave vesicle. The singularity indicator function Δf defined in Eq. (76) is plotted in Fig. 6(a). Two zero positions, which are the solutions of Eq. (76), are marked in Figs. 5 and 6(a) using black squares. The corresponding dielectric energy and interior and exterior Maxwell stresses according to Eqs. (65)–(68) are shown in Figs. 6(b)–6(d). It can be seen that the mutation of dielectric energy and interior and exterior Maxwell stresses are frequency dependent. With an increase of the field frequency, the mutation is weakened, indicating that at high field frequency, the singularity of ac electric fields due to dielectric energy and interior and exterior Maxwell stresses would disappear. It can also be noticed that the singularity at the point near the center, that is, ρ_1 in Fig. 5, is more remarkable. At the far point ρ_2, the mutation is weakened quickly along with an increase of the frequency.

VI. CONCLUSION

In this paper the shape equation for vesicles in an ac electric field has been derived on the basis of the liquid-crystal model. The effects of elastic bending, pressure difference, surface tension, Maxwell pressure, and flexoelectric and dielectric

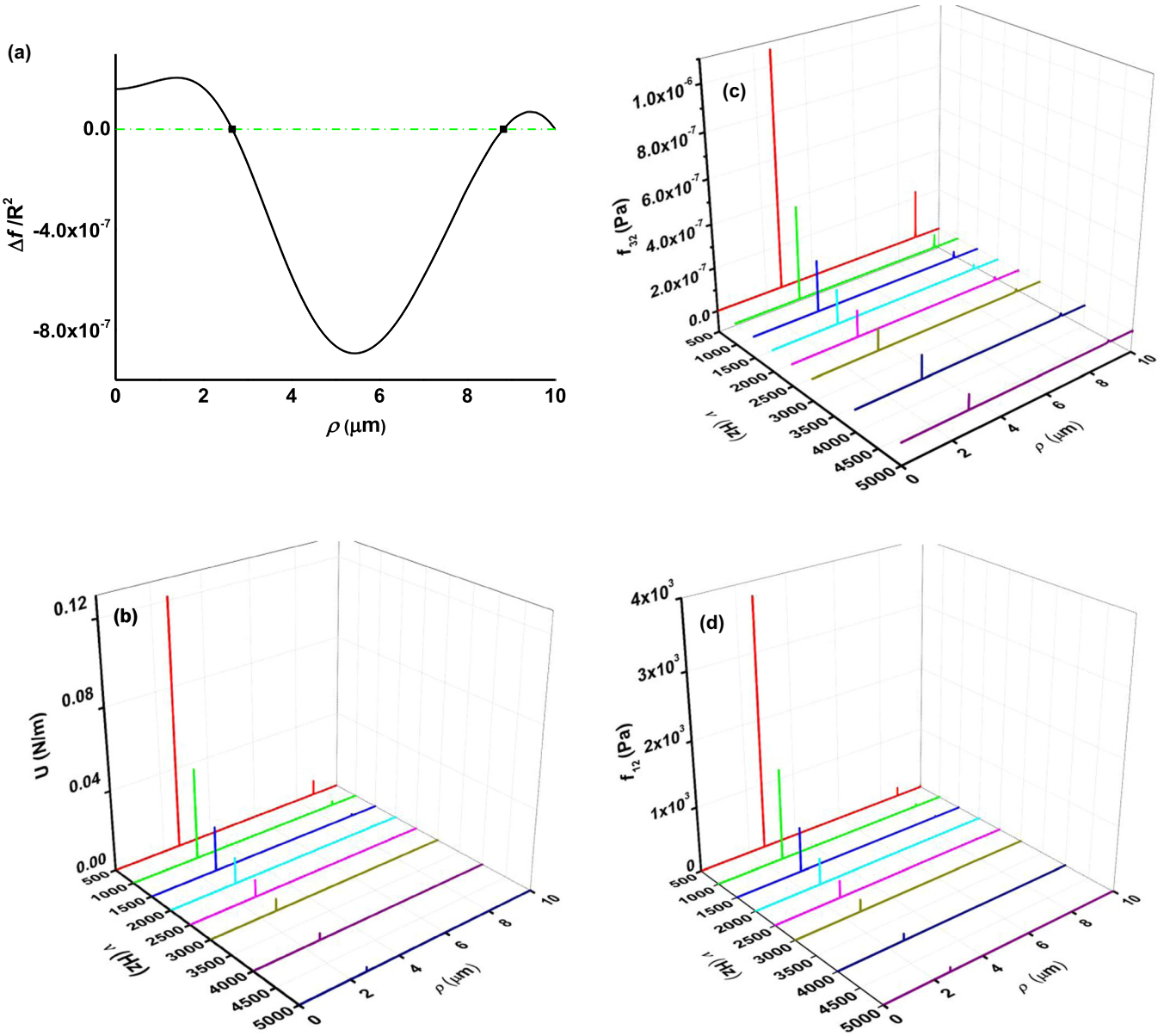

FIG. 6. (Color online) (a) Variation of the singularity indicator function Δf with respect to ρ, (b) variation of the dielectric energy, (c) interior Maxwell pressure, and (d) exterior Maxwell pressure with respect to the field frequency ν and ρ. The parameters used in the calculations are listed in Table I.

properties of the phospholipid membrane were all taken into account in the equation establishment. The shape equation was used to investigate the morphological evolution of vesicles due to an ac electric field. It was found that the shape of a vesicle in an electric field depends not only on its elastic property and the frequency of the applied electric field, but also on the Maxwell pressure, the osmotic pressure difference, and surface tension. The decrease of the pressure difference will increase the critical frequency for the prolate-to-sphere transition, while the increase of surface tension will decrease the frequency for the prolate-sphere-oblate transition. Moreover, the singularity of ac electric field due to dielectric energy and interior and exterior Maxwell stresses is frequency dependent. When the frequency is very high, the singularity would become insignificant. This study helps in the understanding of the frequency-dependent deformation behavior of vesicles and other related phenomena, e.g., electroporation.

ACKNOWLEDGMENTS

Support from the National Natural Science Foundation of China (Grants No. 11272046 and No. 31270989) and the 111 project are acknowledged. Y.-G.T. and Y.L. are grateful for support from the Fundamental Research Funds for the Central Universities of China (Grants No. C14JB00310 and No. 2014JBZ014). Y.L. also acknowledges the support from the Program for New Century Excellent Talents in University (Grant No. NCET-11-0566).

APPENDIX A: COEFFICIENTS A_2, A_3, B_1, AND B_2 IN EQS. (19) AND (20)

The coefficients A_2, A_3, B_1, and B_2 in Eqs. (19)–(22) are derived as

$$A_2 = -3g_0^{-1}E_0(l+d)^3 l\cos\theta\left[\left(l\cos\theta+\frac{dl}{d\theta}\sin\theta\right)+\beta_3\left(2l\cos\theta-\frac{dl}{d\theta}\sin\theta\right)\right], \tag{A1}$$

$$A_3 = -9g_0^{-1}E_0\beta_3(l+d)^3 l^2\cos^2\theta, \tag{A2}$$

$$B_2 = 3g_0^{-1}E_0(l+d)^3 l^4\cos\theta(1-\beta_3)\left(l\cos\theta+\frac{dl}{d\theta}\sin\theta\right), \tag{A3}$$

$$\begin{aligned} B_1 = -g_0^{-1}\Bigg\{ & E_0(1-\beta_1)(l+d)^6\left(l\cos\theta+\frac{dl}{d\theta}\sin\theta\right)\left[\left(l\cos\theta+\frac{dl}{d\theta}\sin\theta\right)+\beta_3\left(2l\cos\theta-\frac{dl}{d\theta}\sin\theta\right)\right] \\ & +E_0 l^3(l+d)^3(\beta_3-1)\left(l\cos\theta+\frac{dl}{d\theta}\sin\theta\right)\left[\left(l\cos\theta+\frac{dl}{d\theta}\sin\theta\right)+\beta_1\left(2l\cos\theta-\frac{dl}{d\theta}\sin\theta\right)\right]\Bigg\}, \end{aligned} \tag{A4}$$

where

$$g_0 = g_1+g_2+g_3+g_4, \tag{A5}$$

$$g_1 = d(3l^2+3ld+d^2)\left(2l\cos\theta-\frac{dl}{d\theta}\sin\theta\right)\left(l\cos\theta+\frac{dl}{d\theta}\sin\theta\right), \tag{A6}$$

$$g_2 = (l+d)^3\left[\beta_3\left(2l\cos\theta-\frac{dl}{d\theta}\sin\theta\right)^2+\beta_1\left(l\cos\theta+\frac{dl}{d\theta}\sin\theta\right)^2\right], \tag{A7}$$

$$g_3 = (\beta_3+\beta_1)l^3\left(2l\cos\theta-\frac{dl}{d\theta}\sin\theta\right)\left(l\cos\theta+\frac{dl}{d\theta}\sin\theta\right), \tag{A8}$$

$$g_4 = \beta_1\beta_3 d(3l^2+3ld+d^2)\left(2l\cos\theta-\frac{dl}{d\theta}\sin\theta\right)\left(l\cos\theta+\frac{dl}{d\theta}\sin\theta\right). \tag{A9}$$

APPENDIX B: COEFFICIENTS D_1, D_{21}, D_{22}, D_{23}, D_3, AND D_4 IN EQ. (47)

The coefficients D_1, D_{21}, D_{22}, D_{23}, D_3, and D_4 in Eq. (47) are given as

$$\begin{aligned} D_1 = {} & \sin^2\theta\cos\theta\left(\frac{dl}{d\theta}\right)^9+l\sin^2\theta\left(\frac{dl}{d\theta}\right)^8+l^2(5\cos\theta-4\cos^3\theta)\left(\frac{dl}{d\theta}\right)^7 \\ & +2l^3\sin\theta(8-7\cos^2\theta)\left(\frac{dl}{d\theta}\right)^6+l^4\cos\theta(17-14\cos^2\theta)\left(\frac{dl}{d\theta}\right)^5+l^5\sin\theta(7\cos^2\theta-3)\left(\frac{dl}{d\theta}\right)^4 \\ & +l^6\cos\theta(16-13\cos^2\theta)\left(\frac{dl}{d\theta}\right)^3+2l^7\sin\theta\cos^2\theta\left(\frac{dl}{d\theta}\right)^3+l^8\cos\theta(3-2\cos^2\theta)\frac{dl}{d\theta}, \end{aligned} \tag{B1}$$

$$\begin{aligned} D_{21} = {} & l^2\sin\theta\Bigg[-(4\cos^2\theta-5)\left(\frac{dl}{d\theta}\right)^6+6l\sin\theta\cos\theta\left(\frac{dl}{d\theta}\right)^5+l^2(42\cos^2\theta-41)\left(\frac{dl}{d\theta}\right)^4 \\ & -2l^3\sin\theta\cos\theta\left(\frac{dl}{d\theta}\right)^3-l^4(9\cos^2\theta-8)\left(\frac{dl}{d\theta}\right)^2-8l^5\sin\theta\cos\theta\frac{dl}{d\theta}-l^6\cos^2\theta\Bigg], \end{aligned} \tag{B2}$$

$$D_{22} = 2l^3\sin^3\theta\left[-9\left(\frac{dl}{d\theta}\right)^4+17l^2\left(\frac{dl}{d\theta}\right)^2-l^4\right]-7l^4\sin^2\theta\cos\theta\frac{dl}{d\theta}\left[l^2+\left(\frac{dl}{d\theta}\right)^2\right], \tag{B3}$$

$$D_{23} = 3l^4\sin^3\theta\left[5\left(\frac{dl}{d\theta}\right)^2-l^2\right], \tag{B4}$$

$$D_3 = 2l^3\sin^2\theta\left[l^3\cos\theta+l\left(\frac{dl}{d\theta}\right)^2\cos\theta+3\sin\theta\left(\frac{dl}{d\theta}\right)^3-l\sin\theta\frac{dl}{d\theta}\left(2l+5\frac{d^2l}{d\theta^2}\right)\right]\left[l^2+\left(\frac{dl}{d\theta}\right)^2\right], \tag{B5}$$

$$D_4 = l^4\sin^3\theta\left[\left(\frac{dl}{d\theta}\right)^4+2l^2\left(\frac{dl}{d\theta}\right)^2+l^4\right]. \tag{B6}$$

[1] S. Aranda *et al.*, Biophys. J. **95**, L19 (2008).
[2] M. Zhao *et al.*, J. Cell Sci. **117**, 397 (2004).
[3] M. B. Zhao *et al.*, Nature (London) **442**, 457 (2006).
[4] J. C. Weaver, J. Cell Biochem. **51**, 426 (1993).
[5] Chen *et al.*, Med. Biol. Eng. Comput. **44**, 5 (2006).
[6] S. Kakorin, T. Liese, and E. Neumann, J. Phys. Chem. B **107**,10243 (2003).
[7] M. M. Sadik *et al.*, Phys. Rev. E **83**, 066316 (2011).
[8] K. A. Riske and R. Dimova, Biophys. J. **88**, 1143 (2005).
[9] T. H. Fan and A. G. Fedorov, Langmuir **19**, 10930 (2003).
[10] H. Hyuga, K. Kinosita, Jr., and N. Wakabayashi, Jpn J. Appl. Phys. **30**, 1141 (1991).
[11] H. Hyuga, K. Kinosita, Jr., and N. Wakabayashi, Jpn. J. Appl. Phys. **30**, 1333 (1991).
[12] M. Winterhalter and W. Helfrich, J. Colloid Interface Sci. **122**, 583 (1988).
[13] P. Peterlin, J. Biol. Phys. **36**, 339 (2010).
[14] P. Peterlin, S. Svetina, and B. Zeks, J. Phys. Condens. Matter. **19**, 136220 (2007).
[15] T. Yamamoto *et al.*, Langmuir **26**, 12390 (2010).
[16] A. D. Rey, Soft Matter **6**, 3402 (2010).
[17] S. J. Singer and G. L. Nicolson, Science **175**, 720 (1972).
[18] H. B. Glenn and J. J. Wolken, *Liquid Crystals and Biological Structures* (Academic, New York, 1979).
[19] A. G. Petrov, *The Lyotropic States of Matter: Molecular Physics and Living Matter Physics* (Gordon & Breach, New York, 1999).
[20] P. G. de Gennes and J. Prost, *The Physics of Liquid Crystals*, 2nd ed. (Oxford University Press, London, 1993).
[21] Z. C. Tu and Z. C. Ou-Yang, Phys. Rev. E **68**, 061915 (2003).
[22] Z. C. Tu and Z. C. Ou-Yang, J. Phys. A **37**, 11407 (2004).
[23] Z. C. Tu, L. Q. Ge, and Z. C. Ou-Yang, Thin Solid Films **509**, 58 (2006).
[24] W. Helfrich, Z. Naturforsh. C. J. Biosci. C **28**, 693 (1973).
[25] L. T. Gao *et al.*, J. Mech. Phys. Solids **56**, 2844 (2008).
[26] L. T. Gao, X. Q. Feng, and H. J. Gao, J. Comput. Phys. **228**, 4162 (2009).
[27] J. Hu and Z. C. Ou-Yang, Phys. Rev. E **47**, 461 (1993).
[28] Z. C. Ou-Yang and W. Helfrich, Phys. Rev. A **39**, 5280 (1989).
[29] J. T. Schwalbe, P. M. Vlahovska, and M. J. Miksis, Phys. Rev. E **83**, 046309 (2011).
[30] H. Hyuga, K. Kinosita, Jr., and N. Wakabayashi, Jpn. J. Appl. Phys. **30**, 2649 (1991).
[31] Z. C. Ou-Yang, J. X. Liu, and Y. Z. Xie, *Geometric Methods in the Elastic Theory of Membranes in Liquid Crystal Phases* (World Scientific, Singapore, 1999).
[32] J. C. Weaver, IEEE Trans. Dielectr. Electr. Insul. **10**, 754 (2003).
[33] D. C. Chang and T. S. Reese, Biophys. J. **58**, 1 (1990).
[34] Q. H. Liu *et al.*, Phys. Rev. E **60**, 3227 (1999).